Heart Surgery Forum 2025; 28(5): E382–E392
doi: 10.59958/hsf.8429

Article

Independent Risk Factors and Surgical Considerations in the Comprehensive Treatment of Coronary Artery Lesions in Pediatric Patients With Kawasaki Disease

Bin Wu[1,*]

[1]Department of Clinical Immunology, Anhui Provincial Children's Hospital, 230051 Hefei, Anhui, China
*Correspondence: wubin80525514@gmail.com (Bin Wu)

Submitted: 20 January 2025 Revised: 6 April 2025 Accepted: 9 May 2025 Published: 27 May 2025

Abstract

Objective: This study aimed to identify independent risk factors for coronary artery lesions (CALs) in Kawasaki disease (KD) patients and evaluate digital subtraction angiography (DSA) as a tool for early detection and individualized management of medium-to-large coronary aneurysms. **Methods**: We selected 206 children diagnosed with KD and 12 who underwent DSA in Anhui Children's Hospital from May 2021 to November 2024. Among the children with KD, 138 were classified into the CALs group and 68 into the non-coronary artery lesions (nCALs) group. SPSS 28.0 and R 3.6.0 were used for statistical analysis. Continuous variables were compared using a *t*-test or Mann–Whitney U test, and categorical variables were compared with the chi-square test or Fisher's exact test. Multivariate logistic regression analysis was used to find independent risk factors for CAL. **Results**: Among the 206 KD patients, the group with CALs (67%) was predominantly male ($p = 0.014$). Elevated white blood cell count (WBC), α-hexadecanoic acid dehydrogenase (α-HBDH), alanine aminotransferase (ALT), ferritin, tumor necrosis factor-alpha (TNF-α), N-terminal pro-brain natriuretic peptide (NT-proBNP), and troponin were observed ($p < 0.05$), alongside increased limb lead low voltage ($p = 0.003$). Multivariate regression analysis confirmed that these indicators were independent risk factors. The area under the curve (AUC) for α-HBDH in predicting CALs was 0.656, with a sensitivity of 33.8% and a specificity of 91.3% at a cutoff value of 146.5 U/L. Restricted cubic spline and decision curve analysis further verified the clinical decision-making value of α-HBDH. DSA provided an accurate assessment of the extent of coronary artery dilation in children. **Conclusion**: This study confirmed that the male sex, white blood cell count, α-HBDH, ferritin, TNF-α, NT-proBNP, and troponin are independent risk factors for KD combined with CALs; meanwhile, α-HBDH exhibited high specificity, with a cutoff value of 146.5 U/L, and the nonlinear relationship and decision curve analysis showed that α-HBDH has good clinical decision-making value within the risk threshold range of 0.3–0.9. DSA can accurately evaluate the inner diameter of coronary arteries and hemodynamics, providing a strong basis for individualized management and treatment strategies for high-risk children. These findings can strengthen the early risk stratification of children with KD combined with CALs and guide the development of individualized treatment plans.

Keywords

coronary artery disease; Kawasaki disease; risk factors; biomarkers; digital subtraction angiography; early diagnosis

Introduction

Kawasaki disease (KD) is an acute systemic vasculitis that primarily affects children aged under five years and is a leading cause of acquired heart disease in pediatric populations worldwide [1]. The most serious complication associated with KD is coronary artery lesions (CALs), which can progress to myocardial infarction, heart failure, or even death if not identified and treated promptly. Although intravenous immunoglobulin (IVIG) therapy significantly reduces the incidence of CALs, approximately 10–20% of patients exhibit resistance to IVIG and remain at elevated risk of coronary artery damage [2]. Given the persistent risk of CALs despite standard therapy, early and accurate imaging assessments are essential for further management.

Currently, the clinical assessment of CALs primarily relies on measuring the inner diameter of the coronary artery, with digital subtraction angiography (DSA) recognized as the gold standard for precise diagnosis. During the early recovery phase, 2–3 months after onset, doctors should use DSA for patients with giant coronary aneurysms or complex medium-sized aneurysms to accurately identify the detailed morphology, location, and extent of the lesions. This thorough evaluation enables clinicians to customize long-term therapeutic approaches and follow-up plans. Moreover, this assessment may help detect CALs early and avoid the use of invasive procedures, such as percutaneous coronary intervention (PCI) and coronary artery bypass grafting (CABG) [3].

However, several knowledge gaps remain. Indeed, existing studies have yet to fully clarify the independent clinical and laboratory predictors of coronary artery dilation in KD, particularly in patients with atypical presentations, such as infants aged under 6 months and children over 5 years, who are more prone to delayed diagnosis and worse outcomes [4]. Furthermore, while inflammatory markers such as C-reactive protein (CRP) and erythrocyte sedimentation rate (ESR) have been linked to severe CALs, the predictive specificity of these markers remains uncertain [5]. Meanwhile, emerging biomarkers, such as troponin, creatine kinase isoenzyme (CK-MB), and N-terminal pro-brain natriuretic peptide (NT-proBNP), have shown potential but require further validation for routine clinical use [6].

The clinical characteristics and laboratory indicators of patients with KD were analyzed to identify independent predictors of coronary artery dilation. Notably, high-risk patients were identified early by combining these predictors with subsequent DSA results. Therefore, this research focused on identifying dependable early indicators for CALs while confirming DSA as a personalized assessment approach to improve risk stratification accuracy and optimize treatment plans for KD patients. This approach can facilitate the proactive management of coronary artery aneurysms and help improve the overall prognosis of affected patients.

Methods

This study included children diagnosed with KD at the Children's Hospital between May 2021 and November 2024.

Inclusion Criteria

- The diagnosis meets the criteria of the Evidence-Based Guidelines for the Diagnosis and Treatment of Kawasaki Disease in Chinese Children (2023) [7].
- Children diagnosed with KD for the first time.
- Parents signed an informed consent form to agree to the study.
- The medical history, laboratory tests, and echocardiography examination data of the patient were complete.

Exclusion Criteria

- Use of immunosuppressive drugs or glucocorticoids before the KD diagnosis.
- Incomplete medical history data.
- Discovery of a cardiovascular disease, genetic metabolic disease, or primary disease other than KD.
- Children in the recovery period of KD, suspected KD, and recurrent KD.

Study Group

As a national medical regional center, our hospital treats various forms of KD, including severe cases. Therefore, we enrolled 206 children with KD and classified them into two groups: those with CALs and those without non-coronary artery lesions (nCALs). The CAL group formed the experimental group and comprised 138 patients, while the nCAL group was the control group and included 68 patients without evidence of coronary artery disease.

Data Collection

Clinical and laboratory data were collected from patient records, including demographic information, medical history, laboratory test results, and echocardiographic findings. Laboratory parameters, including several inflammatory markers (C-reactive protein, white blood cell count(s), etc.), myocardial enzymes (creatine kinase-MB, troponin, etc.), and other necessary biochemical parameters, were evaluated using blood tests. In addition, echocardiography was used to assess coronary artery dimensions and to identify any lesions in these vessels.

Statistical Analysis

Statistical analyses were performed using IBM SPSS Statistics for Windows, version 28.0 (IBM Corp., Armonk, NY, USA) and R software, version 3.6.0 (R Foundation for Statistical Computing, Vienna, Austria).

Quantitative data: The normality of the measured data was assessed using the Shapiro–Wilk test. Data conforming to a normal distribution were presented as the mean ± standard deviation ($\bar{x} \pm s$), and the intergroup comparison was conducted using the independent sample *t*-test. For the non-normally distributed variables, data were expressed as a median and interquartile range [M (IQR)], and differences between the groups were assessed using the Mann–Whitney U test.

Categorical data: Categorical variables are presented as frequencies and percentages. The chi-square test was used for group comparisons; however, if the expected frequency in any cell fell below 5, Fisher's exact probability method was applied instead. Initially, univariate logistic regression analysis was performed to identify potential risk factors. Variables with a p-value <0.05 were subsequently included in the multivariate logistic regression model to ascertain independent predictors of coronary artery disease. The odds ratio (OR) and 95% confidence interval (CI) were calculated for each variable.

Table 1. Comparison of general characteristics between the nCAL and CAL groups.

Parameter	nCAL group (n = 68)	CAL group (n = 138)	Test statistic	*p*-value
Gender, n (%)			$\chi^2 = 6.093$	0.014*
Female	40 (59%)	56 (41%)		
Male	28 (41%)	82 (59%)		
Age, median (IQR), years	1 (1–1)	1 (1–3)	U = 4405	0.415
Fever duration, median (IQR), days	6 (4–7)	5 (4–7)	U = 5188	0.128
Classification, n (%)			$\chi^2 = 0.030$	0.864
Complete type	48 (71%)	99 (72%)		
Incomplete type	20 (29%)	39 (28%)		
Rash, n (%)			$\chi^2 = 0.154$	0.695
With rash	31 (46%)	59 (43%)		
Without rash	37 (54%)	79 (57%)		
Desquamation, n (%)			$\chi^2 = 3.550$	0.060
With desquamation	12 (18%)	12 (9%)		
Without desquamation	56 (82%)	126 (91%)		
Strawberry tongue, n (%)			$\chi^2 = 2.020$	0.155
With strawberry tongue	11 (16%)	13 (9%)		
Without strawberry tongue	57 (84%)	125 (91%)		
Lip redness, n (%)			$\chi^2 = 3.150$	0.076
With lip redness	11 (16%)	11 (8%)		
Without lip redness	57 (84%)	127 (92%)		
Conjunctival congestion, n (%)			$\chi^2 = 0.440$	0.507
With congestion	25 (37%)	44 (32%)		
Without congestion	43 (63%)	94 (68%)		

Note: *$p < 0.05$ indicates statistical significance. Categorical variables were compared using the chi-square test (χ^2); continuous variables were compared using the Mann–Whitney U test. IQR, interquartile range; CAL, coronary artery lesion; nCAL, non-coronary artery lesion.

Results

Comparison of General Characteristics Between the CAL and nCAL Groups

This study comprised 206 pediatric patients with KD, including 68 (33%) in the nCAL group and 138 (67%) in the CAL group. The median age of patients in both groups was 1 year. The gender distribution was significantly different between the two groups ($p < 0.05$), indicating that male pediatric KD patients are more likely to develop CALs (Table 1).

Comparative Analysis of Echocardiographic, Electrocardiographic, and Biochemical Findings Between nCAL and CAL Groups

Analysis of the blood samples showed significant differences in WBC count, ferritin, tumor necrosis factor-α (TNF-α), NT-proBNP, troponin, ALT, and α-hexadecanoic acid dehydrogenase (α-HBDH) between the nCAL and CAL groups, with *p*-values <0.05. These differences indicate the potential of these markers to predict the development of CALs in KD patients. Conversely, PLT counts and other laboratory markers, such as interleukin 1β (IL-1β) and CRP, did not differ significantly between the two groups ($p > 0.05$). The results of the detailed comparisons are presented in Tables 2a,2b.

The electrocardiogram (ECG) analysis also revealed statistically significant differences in the presence of low-voltage limb leads between the two groups ($p = 0.003$), with a notably higher frequency observed in the CAL group. However, other echocardiographic and electrocardiographic indicators did not present significant differences. These findings are summarized in Table 2c.

Multivariate Logistic Regression Analysis of Risk Factors for CAL

This study used multivariate logistic regression analysis to identify key risk factors for CALs in children with KD (Table 3). The data showed boys were 2.469 times more likely to develop CALs than girls. Meanwhile, for every unit increase in α-HBDH, the risk of CALs increased by 0.9%, while for every unit increase in white blood cell count, the risk of CALs increased by 6.2%. Ferritin (ng/mL): For every unit increase, the likelihood of CALs increased by 1.5% (OR = 1.015, $p = 0.0072$). TNF-α (pg/mL): For every unit increase, the likelihood of

Table 2a. Comparison of laboratory test results between the nCAL and CAL groups.

Parameter	nCAL group (n = 68)	CAL group (n = 138)	U-value	*p*-value
	Median (IQR)	Median (IQR)		
Platelet count ($\times 10^9$/L)	415 (318.5, 476.75)	429 (337.0, 527.5)	4122.5	0.157
LDH (U/L)	268 (230.5, 303.0)	278 (249.5, 342.0)	3958.5	0.068
α-HBDH (U/L)	175 (135.0, 250.0)	198 (167.0, 277.5)	3229.5	<0.001 *
CK-MB (U/L)	21 (16.75, 28.25)	21 (16.0, 31.0)	4451.5	0.550
CK (U/L)	42.5 (31.0, 56.0)	40.5 (29.0, 58.0)	4274.5	0.883
WBC ($\times 10^9$/L)	11.2 (8.05, 15.73)	13.5 (9.96, 17.80)	3760.0	0.021 *
NEU ($\times 10^9$/L)	0.55 (0.38, 0.68)	0.61 (0.42, 0.73)	4075.5	0.126
LYM ($\times 10^9$/L)	0.33 (0.23, 0.47)	0.30 (0.22, 0.43)	4167.5	0.437
MONO ($\times 10^9$/L)	0.08 (0.06, 0.11)	0.07 (0.05, 0.10)	5204.0	0.202
RBC ($\times 10^{12}$/L)	4.09 (3.81, 4.33)	4.01 (3.71, 4.35)	5012.0	0.427
AST (U/L)	25 (18.0, 33.25)	23 (16.0, 31.5)	4926.5	0.610
ALT (U/L)	16 (11.0, 27.0)	14 (11.0, 17.75)	4017.0	0.012 *
ALP (U/L)	164.5 (130.75, 196.25)	177.0 (133.25, 216.5)	4083.0	0.143
ESR (mm/h)	66 (41.0, 91.25)	72 (43.0, 93.0)	4441.5	0.534
CRP (mg/L)	53.72 (41.69, 69.53)	57.31 (47.67, 95.41)	4074.5	0.125
PCT (ng/mL)	0.57 (0.18, 1.80)	0.58 (0.23, 2.12)	4298.0	0.328
IL-6 (pg/mL)	37.8 (3.54, 76.75)	53.4 (11.71, 136.57)	4005.2	0.208
TNF-α (pg/mL)	20.1 (13.2, 27.5)	28.9 (18.5, 68.3)	3108.0	0.021 *
IL-1β (pg/mL)	22.0 (18.1, 27.3)	24.5 (19.0, 30.6)	4500.0	0.267

Note: * indicates $p < 0.05$. Abbreviations: LDH, lactate dehydrogenase; α-HBDH, α-hydroxybutyrate dehydrogenase; CK-MB, creatine kinase isoenzyme; WBC, white blood cell count; NEU, neutrophils; LYM, lymphocytes; MONO, monocytes; RBC, red blood cell count; AST, aspartate transaminase; ALT, alanine transaminase; ALP, alkaline phosphatase; ESR, erythrocyte sedimentation rate; CRP, C-reactive protein; PCT, procalcitonin; IL, interleukin; TNF, tumor necrosis factor.

Table 2b. Comparison of biochemical markers between the nCAL and CAL groups.

Biochemical marker	nCAL group (n = 68)	CAL group (n = 138)	*t*-value	*p*-value
Ferritin (ng/mL)	184.53 ± 14.27	235.69 ± 23.57	–2.68	0.008*
IL-2R (U/mL)	5476 ± 1976	5172 ± 1672	1.04	0.298
NT-proBNP (pg/mL)	496.75 ± 95.23	562.73 ± 104.31	–2.05	0.042*
Troponin (ng/mL)	1.09 ± 0.35	1.73 ± 0.38	–4.38	<0.001*

Note: *$p < 0.05$ indicates statistical significance. NT-proBNP, N-terminal pro-brain natriuretic peptide.

Table 2c. Echocardiography and electrocardiogram (EKG) findings in nCAL and CAL groups.

Parameter	nCAL group (n = 68)	CAL group (n = 138)	*p*-value
Echocardiography			
Left ventricular dilation	1 (1.5%)	4 (2.9%)	1.000
Left ventricular systolic dysfunction	2 (2.9%)	4 (2.9%)	1.000
EKG			
Limb lead low voltage	2 (2.9%)	24 (17.1%)	0.003 *
Atrioventricular block	2 (2.9%)	5 (3.6%)	1.000

Note: *$p < 0.05$ indicates statistical significance. The low voltage in the limb leads was statistically significant with a *p*-value of 0.003.

CALs increased by 3.2% (OR = 1.032, $p = 0.0275$). NT-proBNP (pg/mL): For every unit increase, the likelihood of CALs increased by 0.6% (OR = 1.006, $p = 0.0283$). Troponin (ng/mL): Each unit increase was associated with a 72.3% increased likelihood of CALs (OR = 1.723, $p <$ 0.001). These findings suggest that elevated levels of these biomarkers are strongly associated with an increased risk of CALs in children with KD.

Table 3. Multivariate logistic regression analysis of risk factors for CALs.

Factor	Estimate	Std. error	Z-value	*p*-value	OR	95% CI
Male	0.903956	0.316946	2.852	0.00434 *	2.469	1.327–4.596
α-HBDH	0.008545	0.003243	2.635	0.00841 *	1.009	1.002–1.015
WBC	0.060184	0.028119	2.140	0.03232 *	1.062	1.005–1.122
Ferritin (ng/mL)	0.0145	0.0054	2.690	0.0072 *	1.015	1.004–1.027
TNF-α (pg/mL)	0.0312	0.0141	2.210	0.0275 *	1.032	1.004–1.061
NT-proBNP (pg/mL)	0.0057	0.0026	2.190	0.0283 *	1.006	1.000–1.013
Troponin (ng/mL)	0.5438	0.1257	4.330	<0.001 *	1.723	1.335–2.226

Note: *$p < 0.05$ indicates statistical significance. $p < 0.05$ indicates statistical significance.

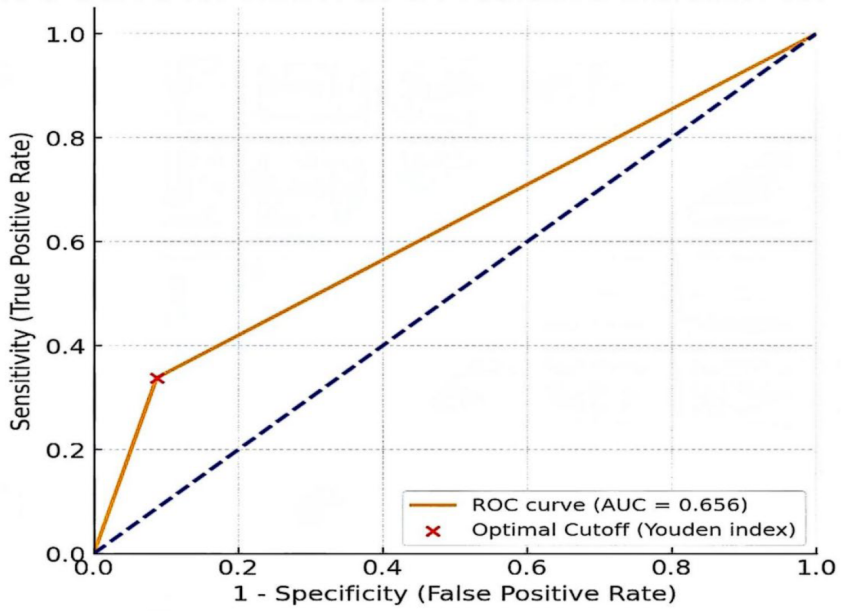

Fig. 1. ROC curve of α-HBDH for the prediction of CALs. α-HBDH, α-hexadecenoic acid dehydrogenase; CALs, coronary artery lesions; ROC, receiver operating characteristic; AUC, area under the curve.

Predictive Value of α-HBDH for CALs

The receiver operating characteristic (ROC) curve analysis showed that the predictive ability of α-HBDH for CALs was moderate, with an AUC value of 0.656 (95% CI: 0.5749–0.7368). Subsequently, taking the optimal cutoff value of α-HBDH of 146.5 U/L as the standard produced a sensitivity value of 33.8% and a specificity of 91.3%. This result shows that although α-HBDH has a high specificity in distinguishing CAL patients from non-CAL patients, its sensitivity is low, meaning it can better exclude non-CAL cases (Fig. 1).

Fig. 2 presents the analysis of sophisticated statistical tools, such as restricted cubic spline models, which show that the relationship between α-HBDH levels and risk of CALs is not linear. Indeed, the risk of developing CALs increases at lower α-HBDH concentrations, but it is a slow rise. However, as α-HBDH levels increase, the risk increases more rapidly and by a more significant amount. This pattern suggests that higher α-HBDH concentrations substantially affect the risk of CALs more than having the same impact at every level. The threshold effect shows that the risk of CALs spikes at a certain point in α-HBDH values. This means there is a predictive value for CALs after studying α-HBDH up to a specific value. The dose–response relationship with a *p*-value of 0.015 means that the association between α-HBDH levels and CAL risk is statistically significant and not coincidental.

Decision Curves for α-HBDH and CALs

Fig. 3 shows the decision curve analysis (DCA) results of a univariate logistic regression model using α-HBDH as a predictor to assess the risk of CALs in patients with KD or similar diseases. The data were from patients with KD, where α-HBDH levels were measured in the acute phase, and the occurrence of CALs was confirmed using diagnostic methods such as echocardiography. The univariate logistic regression was employed as the statistical method, which uses the following formula to estimate the probability of CALs based on the α-HBDH levels:

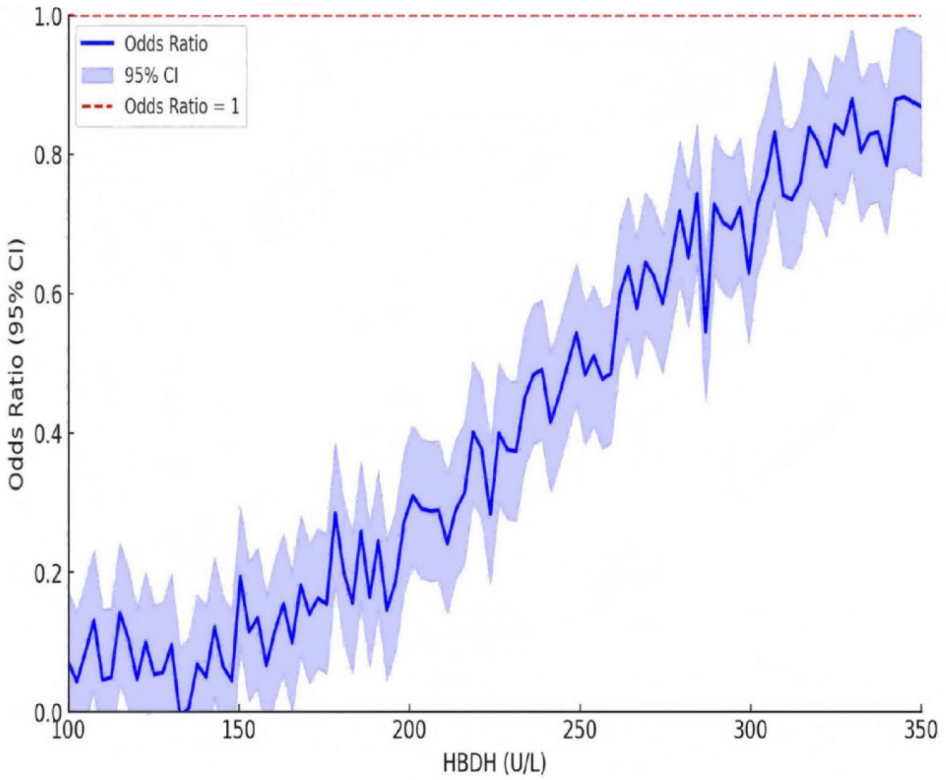

Fig. 2. Dose–response analysis between α-HBDH and CALs based on the restrictive cubic spline mode. 95% CI, 95% confidence interval.

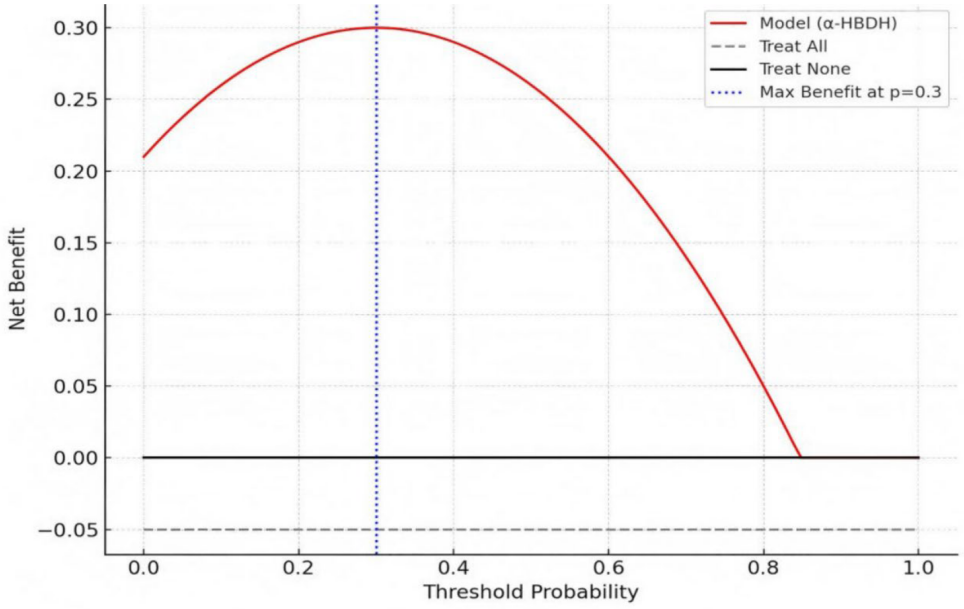

Fig. 3. Decision curve analysis diagram for α-HBDH.

$$P(\mathrm{CAL}) = \frac{1}{1 + \exp\left(-\left(\beta_0 + \beta_1 \cdot \alpha - \mathrm{HBDH}\right)\right)}$$

β_0 represents the intercept, and β_1 is the regression coefficient for α-HBDH; both are determined by fitting the model to the cohort data. This approach isolates the predictive power of α-HBDH, quantifying its direct association with CAL risk without incorporating additional variables. Indeed, by focusing on a single biomarker, the model offers a straightforward tool for clinical risk assessment.

The horizontal axis represents the threshold probability at which the doctor assesses whether the patient is at high risk for CALs; when the doctor believes that the risk of the patient developing CALs is more than 30%, the doctor will consider administering treatment. The vertical axis represents the net clinical benefit, which is the benefit of using this prediction tool to guide decision-making. Here, "clinical benefit" refers to correctly identifying patients who need treatment and avoiding treating patients who do not require intervention. The red curve represents the net clinical benefit of using α-HBDH to predict risk and guide treatment decisions. The height of the red curve shows the clinical benefit of using α-HBDH at different threshold probabilities. The gray dotted line represents the net clinical benefit of the "treat all" strategy: Treating all patients (regardless of risk). This line is usually low because there is no distinction between high-risk and low-risk patients. The black solid line represents the net clinical benefit of the "no treatment" strategy, where no patients are treated regardless of risk. This line is typically flat at zero because no treatment is provided, resulting in no clinical benefit.

As can be seen from the figure, within the threshold probability range of 0.1 to 0.9, the red curve is always higher than the other two lines, indicating that within this interval, using α-HBDH for treatment decision-making has higher clinical benefits than the "treat all" or "treat none" strategies, and has good clinical application value. The peak of the red curve occurs at 0.3 to show that α-HBDH becomes most beneficial for clinical decisions when doctors determine that the risk of CALs in a patient exceeds 30%. α-HBDH provides the best clinical reference between avoiding overtreatment and delayed treatment. Therefore, α-HBDH is considered a valuable indicator, especially in helping doctors decide whether to conduct clinical interventions that bring significant clinical benefits.

Analysis of DSA in Children With Coronary Artery Aneurysm

To evaluate the importance of independent risk factors for CALs in children with KD, we assessed 12 children with coronary artery aneurysms who underwent DSA in our hospital between May 2021 and November 2024. Table 4 summarizes the basic information, the main imaging manifestations of the right and left coronary arteries, and the DSA diagnostic grading for each patient.

The 12 children were aged between 8 months and 10 years. Case 3 had a right coronary artery aneurysm (4.43 mm $\times$ 10.92 mm, Z = 5.44) and a left anterior descending artery aneurysm (3.09 mm $\times$ 6.26 mm, Z = 2.71) on the DSA. Case 4 had a right coronary artery aneurysm (2.73 mm, Z = 3.72) and left coronary artery aneurysm (3.5 mm, Z = 5.36). Case 5 had a right coronary artery aneurysm (5.35 mm, Z = 8.88) and left coronary artery dilatation (4.81 mm, Z = 7.88). Case 9 had a right coronary artery aneurysm (6.3 mm, Z = 9.97) and mild dilatation of the left coronary artery (4.14 mm). In these cases, the degree of dilatation of the coronary artery aneurysms was moderate to severe, and the Z values reflected a significant deviation from the expected values.

Case 1 had grade IV coronary artery dilatation, with the maximum diameter of the right coronary artery aneurysm being 13.19 mm, while the left coronary artery remained normal (2.51 mm). Case 12 had giant aneurysms in both the right coronary (14.06 mm) and left coronary (7.96 mm and 11.20 mm) arteries, partial filling defects, and the right coronary artery had collateral supply. The higher the grade of the lesions, the greater the severity (grade IV, severe). This requires individualized treatment, and surgical treatment can be performed later. Case 6 had two fusiform dilatations in the left anterior descending artery (3.32 mm $\times$ 5.18 mm and 5.79 mm $\times$ 9.12 mm) and was diagnosed as "high risk of thrombosis". Case 7 had a right coronary artery aneurysm (6.18 mm) and a normal left coronary artery (1.57 mm) and was diagnosed with a coronary artery aneurysm. Children with giant aneurysms (cases 1, 12) and high-risk features (case 6, thrombotic risk) are at risk of myocardial infarction, thrombosis, or sudden death. Moderate aneurysms (grade IIIb) require monitoring for progression. Cases with severe findings (e.g., 1, 6, 12) may require aggressive intervention such as anticoagulation medication or surgery, whereas standard cases (e.g., 2, 8, 10) need only routine follow-up.

The DSA results indicated that nine patients exhibited varying degrees of coronary artery dilatation, classified from grade II to severe. The comprehensive images obtained by the DSA can accurately assess the dilatation of coronary arteries in children.

Discussion

Among the 206 children with KD, 67% were diagnosed with CALs, with the highest proportion noted in the male children (p = 0.014). The WBC, α-HBDH, TNF-α, NT-proBNP, and troponin levels were elevated ($p <$ 0.05), while the electrocardiogram limb lead voltage was decreased (p = 0.003). Multivariate regression analysis confirmed that these biomarkers were independent risk factors for CALs. Restricted cubic spline analysis and decision curve analysis further validated the clinical utility of α-HBDH, while DSA could accurately assess coronary artery dilatation.

In the sex-specific gene analysis, six susceptibility loci (*PDE1C*, *NOS3*, *DLG2*, *CPNE8*, *FUNDC1*, and *GABRQ*) were associated with CALs in boys, while two genes (*SMAD3* and *IL1RAPL1*) were associated with CALs in girls [8]. Previous studies have shown that male mice have more severe coronary artery inflammation and dilation after KD induction, which may be related to increased expressi-

Table 4. DSA manifestations of coronary artery disease in children.

Case	Sex	Age	Right coronary description	Left coronary description	DSA Dx	Treatment	Follow-up status
1	M	4 yrs	Significant dilation at the origin of the main trunk; maximum coronary aneurysm diameter 13.19 mm	Main trunk not dilated, inner diameter ~2.51 mm; left circumflex and anterior descending branches well displayed	Coronary lesions (grade IV)	Oral aspirin, metoprolol, and warfarin	Stable, no thrombosis, regular monitoring
2	M	3 yrs	No dilation throughout; inner diameter: proximal 2.05 mm, mid-segment 1.79 mm, distal 1.69 mm	No dilation throughout; main trunk inner diameter ~2.05 mm; other branches normal	Normal coronary arteries	Regular cardiac ultrasound examination	No coronary artery disease developed
3	F	7 yrs	Significant dilation in the proximal–mid segment of the main trunk; aneurysm size ~4.43 mm × 10.92 mm (Z = 5.44)	Left main trunk essentially normal; aneurysmal dilation at the origin of the left anterior descending branch (~3.09 mm × 6.26 mm, Z = 2.71)	Coronary lesions (grade IIIb)	Dual anticoagulation therapy with aspirin and clopidogrel	Stable, mild dilation persists, no progression
4	M	8 m 16 d	Aneurysm formation in the main trunk and proximal segment, widest part ~2.73 mm (Z = 3.72); aneurysm length ~12.35 mm	Aneurysm formation from main trunk to bifurcation, widest part ~3.5 mm (Z = 5.36)	Coronary lesions (grade IIIb)	Dual anticoagulation therapy with aspirin and clopidogrel	Postoperative recovery, no further dilation
5	F	6 yrs	Significant dilation of the main trunk; coronary aneurysm inner diameter ~5.35 mm (Z = 8.88), length ~11.07 mm	Mild dilation of the main trunk and left circumflex (inner diameters ~4.19 mm and 3.11 mm); left anterior descending inner diameter ~4.81 mm (Z = 7.88)	Coronary lesions (grade IIIb)	Dual anticoagulation therapy with aspirin and clopidogrel	Improvement, reduced dilation, under close monitoring
6	M	6 yrs	Right coronary description not specifically provided	Left coronary shows two fusiform dilations in mid-segment of left anterior descending branch (~3.32 mm × 5.18 mm and 5.79 mm × 9.12 mm), suggesting high risk of thrombosis	High risk of thrombosis	Oral treatment with rivaroxaban, aspirin, and metoprolol	High risk persists, further intervention planned
7	F	9 m 29 d	Significant dilation at origin of main trunk; coronary aneurysm diameter ~6.18 mm, length ~5.11 mm	Main trunk not dilated; inner diameter ~1.57 mm; other branches appear normal	Coronary aneurysm	Stop anticoagulation and recommend surgery	Stable, aneurysm unchanged
8	F	9 yrs	Inner diameters range from 2.12 to 1.18 mm across segments, normal morphology	Inner diameters range from 2.28 to 1.37 mm across segments, normal morphology	No coronary dilation	Stop medication and have regular cardiac ultrasound examinations	No coronary artery disease developed
9	F	4 yrs	Significant dilation at the origin of the main trunk; coronary aneurysm diameter ~6.3 mm (Z = 9.97)	Mild dilation of the main trunk and left circumflex, inner diameter ~4.14 mm; left anterior descending inner diameter ~1.58 mm	Coronary lesions (grade IIIb)	Dual anticoagulation therapy with aspirin and clopidogrel	Stable, no complications, regular follow-up
10	M	10 yrs	No dilation throughout; inner diameter: proximal 2.28 mm, mid-segment 1.61 mm, distal 1.22 mm	No dilation throughout; main trunk inner diameter ~2.59 mm; other branches appear normal	Normal coronary inner diameter	Stop medication and have regular cardiac ultrasound examinations	No coronary artery disease developed
11	M	4 yrs	No dilation throughout; right coronary proximal inner diameter ~2.67 mm, mid-segment ~1.47 mm	No dilation throughout; inner diameter: main trunk 2.38 mm, left circumflex ~1.64 mm, anterior descending ~1.69 mm	Coronary lesions (grade II)	Conservative treatment (aspirin)	Mild disease persists, no progression
12	M	9 yrs	Significant dilation at origin of the main trunk; giant coronary aneurysm diameter ~14.06 mm, length ~20.03 mm; partial filling defect	Giant coronary aneurysms in the left circumflex and left anterior descending branches (inner diameters ~7.96 mm and 11.20 mm), with collateral supply to right coronary	Coronary lesions (severe)	Oral aspirin and metoprolol, recommend surgery	Stable, regular follow-up, under close monitoring

DSA, digital subtraction angiography; d, days; yrs, years; m, months; M, Male; F, Female.

ons of IL-1β and IL-1R1 [9]. This result aligns with the higher incidence of CALs in boys observed in this study. Despite these differences, the current diagnostic criteria for CALs do not consider gender, which may explain the higher diagnosis rate of CALs in boys [10].

The inflammatory response in the acute phase of KD is triggered by activated leukocytes, which release cytokines, such as TNF-α, matrix metalloproteinases, and reactive oxygen species, leading to endothelial dysfunction and vascular damage [11–13]. These mediators promote the degradation of extracellular matrix components, leading to endothelial cell death and aneurysm formation. Activated platelets also promote vascular inflammation by recruiting leukocytes and triggering proinflammatory pathways [14]. Our study found that the leukocyte count was independently associated with the risk of CALs (OR = 1.062). Meanwhile, by tracking leukocyte levels during the acute phase, medical staff can better identify high-risk patients and provide medical intervention earlier. Significantly elevated α-HBDH levels in patients with CALs indicate myocardial or vascular wall cell damage, and α-HBDH levels above 146.5 U/L indicate an increased risk of CALs. Our evidence suggests that α-HBDH may be an effective early biomarker for CALs, especially in ischemia resulting from coronary artery dilatation [15].

Timely administration of IVIG within 7 days of symptom onset significantly reduces the risk of CALs [16]. Patients with incomplete Kawasaki disease (IKD) are at high risk for coronary artery damage because atypical symptoms lead to delayed diagnoses, resulting in persistent vascular inflammation. ECG and echocardiogram evaluations are essential after prompt diagnoses to ensure patients receive the appropriate treatment. Our results suggest that the reduced limb lead voltage observed on the ECGs of patients with CALs may serve as a simple, noninvasive adjunct.

Elevated ferritin levels are associated with CALs, supporting the role of proinflammatory cytokines in the development of CALs [17]. Our study also confirmed the key role of TNF-α in coronary artery inflammation, consistent with previous findings [18]. Biological therapy targeting TNF-α may provide a promising approach to reducing coronary artery damage in patients with KD. Similarly, NT-proBNP levels were significantly increased in patients with CALs, further supporting its role as a marker of coronary artery abnormalities [19]. Our investigation demonstrated elevated troponin levels, which indicate myocardial injury in patients with CALs, indicating myocardial ischemia and validating coronary artery damage, which aligns with previous research by Sato *et al*. [20]. These biomarkers could be incorporated into routine clinical practices to assist in the early detection of CALs and myocardial injury. Although IL-1β is known to play a role in the inflammatory response in KD, our study did not find a significant association between IL-1β levels and CAL formation. This result differs from the study reported by Leung *et al*. [21], who showed that IL-1β could accelerate disease progression. The progression of KD resulted in changes in cytokine expression patterns, which may explain these inconsistent observations. Research must continue to explore how cytokines change over time and their impact on the development of CALs.

Limitations

Most of the research participants originated from Anhui Province in China. These study results may not relate to different regions owing to geographic differences, ethnic diversity, and socioeconomic disparities that affect healthcare access and CAL diagnosis. Patients from wealthier socioeconomic backgrounds tend to access medical care sooner and receive earlier diagnoses, which results in milder symptoms. This research occurred in a tertiary pediatric hospital, which likely caused referral bias and led to more severe cases and higher reported rates of CALs. This retrospective study approach introduced potential biases because of missing or incomplete clinical data. Moreover, due to recall bias, assessing risk factors becomes less accurate when researchers depend on medical records, clinical notes, or parental memories.

Future Research

Future research must encompass multiple medical centers to enlarge the sample size while ensuring patient diversity across different demographics and healthcare settings. Future investigations should use longitudinal research methods to observe CAL progression across long timeframes. Investigations should analyze sex-specific genetic influences on CAL risk while evaluating the potential of α-HBDH as an early detection biomarker for CALs. This study includes an assessment of TNF-α inhibitors for their ability to stop CAL progression. Patient demographics, including sex, age, and genotype, must be used to stratify study populations because CALs demonstrate inherent heterogeneity. The recruitment strategy in this study included gathering participants from multiple medical centers to achieve diverse genetic and demographic representation. This stratified analysis approach requires adequate participant recruitment from diverse backgrounds, such as low and high socioeconomic status, to ensure that the dataset reflects different demographic groups. This study used multivariate regression analysis across multiple subgroups to determine the influence of various factors on CAL risk. Follow-up procedures should consist of clinical evaluations at six-month intervals and again after one year to monitor patient health status, biomarker concentrations, and additional pertinent variables. The progression of CALs should be tracked using high-resolution cardiac CT scans and three-dimensional echocardiography. All imaging assessments should adhere to standardized protocols to maintain con-

sistency and accuracy. Hence, by studying various patient groups, this comprehensive approach can identify specific risk factors that enable the development of personalized treatment strategies, including minimally invasive coronary artery surgery and medical therapies that match the needs of each patient.

Conclusion

This study identified key predictors of CALs in patients with KD, including elevated white blood cell counts, ferritin, TNF-α, NT-proBNP, troponin, and decreased limb lead voltage levels, as well as sex-specific susceptibility associated with genetic factors and the interleukin-1 pathway. In addition, α-HBDH levels above 146.5 U/L emerged as a potential biomarker for severe vascular damage. Echocardiography and DSA can help identify coronary artery abnormalities that may require CABG or PCI and help select arterial grafts that can grow with the child, thereby improving long-term outcomes [22]. These results lay the foundation for updating clinical guidelines to incorporate new biomarkers and imaging indicators into risk-stratification schemes, enabling earlier and more targeted interventions. Future research plans should collaborate with hospitals using advanced diagnostic technologies, such as pediatric coronary angiography, cardiac magnetic resonance imaging, and three-dimensional echocardiography, to conduct multicenter prospective studies and standardized longitudinal data collection to improve data representativeness and completeness. This prospective research method will include stratified analysis of different KD subtypes (including IKD and intravenous immunoglobulin–resistant KD). Moreover, multi-center research can expand population diversity and reduce bias to establish a more complete risk stratification model, achieve more accurate risk prediction for children with CALs, and provide more meaningful clinical guidance for coronary artery surgery.

Availability of Data and Materials

The datasets generated and/or analyzed during the current study are not publicly available due to institutional policies and concerns about patient confidentiality in accordance with ethical guidelines. However, de-identified data may be made available from the corresponding author upon reasonable request and with prior approval from the institutional ethics review board.

Author Contributions

The single author had the sole role in designing, data collecting, analyzing, and writing the manuscript.

Ethics Approval and Consent to Participate

The study was carried out in accordance with the guidelines of the Declaration of Helsinki and approved by the Ethics Committee of Anhui Provincial Children's Hospital (Protocol No. PJ20200103). Written informed consent to participate was obtained from the patient's parent or legal guardian prior to inclusion in the study.

Acknowledgment

Not applicable.

Funding

This research received no external funding.

Conflict of Interest

The author declares no conflict of interest.

References

[1] Selmek K, Harding M. Kawasaki Disease. Pediatrics in Review. 2024; 45: 425–427. https://doi.org/10.1542/pir.2023-006051.

[2] Zhang R, Shuai S, Zhang H, Cai J, Cui N, Tang M, *et al*. Predictive value of albumin for intravenous immunoglobulin resistance in a large cohort of Kawasaki disease patients. Italian Journal of Pediatrics. 2023; 49: 78. https://doi.org/10.1186/s13052-023-01482-z.

[3] Swaye PS, Fisher LD, Litwin P, Vignola PA, Judkins MP, Kemp HG, *et al*. Aneurysmal coronary artery disease. Circulation. 1983; 67: 134–138. https://doi.org/10.1161/01.cir.67.1.134.

[4] Kuo HC. Diagnosis, Progress, and Treatment Update of Kawasaki Disease. International Journal of Molecular Sciences. 2023; 24: 13948. https://doi.org/10.3390/ijms241813948.

[5] Xue M, Wang J. Utility of color Doppler echocardiography combined with clinical markers in diagnosis and prediction of prognosis of coronary artery lesions in Kawasaki disease. Experimental and Therapeutic Medicine. 2020; 19: 2597–2603. https://doi.org/10.3892/etm.2020.8519.

[6] Doros G, Bataneant M, Mihailov D, Popoiu A, Stroescu R, Steflea R, *et al*. Cardiovascular Spectrum and Cardiac Biomarkers in Pediatric Inflammatory Multisystem Syndrome with Kawasaki-Like Disease-Our Experience During the COVID-19 Pandemic in the West Part of Romania. Romanian Journal of Cardiology. 2021; 31: 861–873. https://doi.org/10.47803/rjc.2020.31.4.861.

[7] Center for Diagnosis and Treatment of Kawasaki Disease/Children's Hospital of Shaanxi Provincial People's Hospital, National Children's Medical Center/Beijing Children's Hospital, Capital Medical University, Children's Hospital,Shanghai Jiao Tong University School of Medicine, National Regional Medical Center/Shengjing Hospital of China Medical University, National Clinical Key Specialty/Department of Intensive Care Medicine, Shanghai Children'sHospital, Hospital; General Pediatric Group of Pediatrician Branch of Chinese

Medical Doctor Association, *et al*. Evidence-based guidelines for the diagnosis and treatment of Kawasaki disease in children in China (2023). Zhongguo Dang Dai Er Ke Za Zhi = Chinese Journal of Contemporary Pediatrics. 2023; 25: 1198–1210. https://doi.org/10.7499/j.issn.1008-8830.2309038.

[8] Kim JJ, Hong YM, Yun SW, Lee KY, Yoon KL, Han MK, *et al*. Sex-Specific Susceptibility Loci Associated With Coronary Artery Aneurysms in Patients With Kawasaki Disease. Korean Circulation Journal. 2024; 54: 577–586. https://doi.org/10.4070/kcj.2023.0244.

[9] Porritt RA, Markman JL, Maruyama D, Kocaturk B, Chen S, Lehman TJA, *et al*. Interleukin-1 Beta-Mediated Sex Differences in Kawasaki Disease Vasculitis Development and Response to Treatment. Arteriosclerosis, Thrombosis, and Vascular Biology. 2020; 40: 802–818. https://doi.org/10.1161/ATVBAHA.119.313863.

[10] Kobayashi T, Fuse S, Sakamoto N, Mikami M, Ogawa S, Hamaoka K, *et al*. A New Z Score Curve of the Coronary Arterial Internal Diameter Using the Lambda-Mu-Sigma Method in a Pediatric Population. Journal of the American Society of Echocardiography: Official Publication of the American Society of Echocardiography. 2016; 29: 794–801.e29. https://doi.org/10.1016/j.echo.2016.03.017.

[11] Hara T, Yamamura K, Sakai Y. The up-to-date pathophysiology of Kawasaki disease. Clinical & Translational Immunology. 2021; 10: e1284. https://doi.org/10.1002/cti2.1284.

[12] Kurihara T, Shimizu-Hirota R, Shimoda M, Adachi T, Shimizu H, Weiss SJ, *et al*. Neutrophil-derived matrix metalloproteinase 9 triggers acute aortic dissection. Circulation. 2012; 126: 3070–3080. https://doi.org/10.1161/CIRCULATIONAHA.112.097097.

[13] Scioli MG, Storti G, D'Amico F, Rodríguez Guzmán R, Centofanti F, Doldo E, *et al*. Oxidative Stress and New Pathogenetic Mechanisms in Endothelial Dysfunction: Potential Diagnostic Biomarkers and Therapeutic Targets. Journal of Clinical Medicine. 2020; 9: 1995. https://doi.org/10.3390/jcm9061995.

[14] Totani L, Evangelista V. Platelet-leukocyte interactions in cardiovascular disease and beyond. Arteriosclerosis, Thrombosis, and Vascular Biology. 2010; 30: 2357–2361. https://doi.org/10.1161/ATVBAHA.110.207480.

[15] Shahjehan RD, Sharma S, Bhutta BS. Coronary artery disease. In: StatPearls [Internet]. StatPearls Publishing: Treasure Island (FL). 2024.

[16] Li W, He X, Zhang L, Wang Z, Wang Y, Lin H, *et al*. A Retrospective Cohort Study of Intravenous Immunoglobulin Therapy in the Acute Phase of Kawasaki Disease: The Earlier, the Better?. Cardiovascular therapeutics. 2021; 2021: 6660407. https://doi.org/10.1155/2021/6660407.

[17] Kim SH, Song ES, Yoon S, Eom GH, Kang G, Cho YK. Serum Ferritin as a Diagnostic Biomarker for Kawasaki Disease. Annals of Laboratory Medicine. 2021; 41: 318–322. https://doi.org/10.3343/alm.2021.41.3.318.

[18] Matsubara T, Furukawa S, Yabuta K. Serum levels of tumor necrosis factor, interleukin 2 receptor, and interferon-gamma in Kawasaki disease involved coronary-artery lesions. Clinical Immunology and Immunopathology. 1990; 56: 29–36. https://doi.org/10.1016/0090-1229(90)90166-n.

[19] Jung JH, Hwang S, Jung JY, Park JW, Lee EJ, Lee HN, *et al*. Brain natriuretic peptide as a clinical screening tool for the diagnosis of Kawasaki disease. Medicine. 2023; 102: e34319. https://doi.org/10.1097/MD.0000000000034319.

[20] Sato YZ, Molkara DP, Daniels LB, Tremoulet AH, Shimizu C, Kanegaye JT, *et al*. Cardiovascular biomarkers in acute Kawasaki disease. International Journal of Cardiology. 2013; 164: 58–63. https://doi.org/10.1016/j.ijcard.2011.06.065.

[21] Leung DY, Cotran RS, Kurt-Jones E, Burns JC, Newburger JW, Pober JS. Endothelial cell activation and high interleukin-1 secretion in the pathogenesis of acute Kawasaki disease. Lancet (London, England). 1989; 2: 1298–1302. https://doi.org/10.1016/s0140-6736(89)91910-7.

[22] Kitamura S. A new arena in cardiac surgery: Pediatric coronary artery bypass surgery. Proceedings of the Japan Academy. Series B, Physical and Biological Sciences. 2018; 94: 1–19. https://doi.org/10.2183/pjab.94.001.